5-1-2021

PARAMETRIC SIZING OF A RBCC SSTO SPACE TOURISM VEHICLE

Henry Barahona

PARAMETRIC SIZING OF A RBCC SSTO SPACE TOURISM VEHICLE

by

HENRY J. BARAHONA MIRANDA

Presented to the Faculty of the Honors College of

The University of Texas at Arlington in Partial Fulfillment

of the Requirements

for the Degree of

HONORS BACHELOR OF SCIENCE IN AEROSPACE ENGINEERING

THE UNIVERSITY OF TEXAS AT ARLINGTON

May 2021

ACKNOWLEDGMENTS

First and foremost, I would like to thank God for giving me not only the opportunity to complete my higher education studies in the field that I love, but for also giving me the strengths that I needed every day to work hard and diligently on all my tasks and assignments while keeping me safe, protected, and surrounded by people who love and support me.

Second, I want to thank my faculty mentor, Dr. Bernd Chudoba, for his teaching, advice, encouragement, support, and constructive criticism throughout the entire process. Thank you for always pushing me to my limit, so I could get the maximum benefit out of the experience. Dr. Chudoba made it clear since the very first day that the road was not going to be easy. However, he was always there to provide a new perspective and to get me back on track. Similarly, I would like to thank Ian Maynard for taking the time, out of his busy schedule, to provide me guidance and support when working on this project.

Last but not least, I would like to thank my father, Henry Barahona, my mother, Patricia Miranda, and my sister, Daniela Barahona, with all my heart. Their kind words and their motivational talks were always key in inspiring and reminding me to keep my head up and keep pushing even when times got tough. I definitely would not be where I am today without their entire and unconditional love and support. It was not easy leaving my home, and even my country, to follow my dream. However, I can finally say that this sacrifice has been worth it.

May 3, 2021

ABSTRACT

PARAMETRIC SIZING OF A RBCC SSTO SPACE TOURISM VEHICLE

Henry J. Barahona Miranda, B.S. Aerospace Engineering

The University of Texas at Arlington, 2021

Faculty Mentor: Bernd Chudoba

As of Spring 2021, Virgin Galactic is attempting to become the first company to provide commercial space tourism by starting its two-stage-to-sub-orbit (TSTSO) flight program as early as the first quarter of 2022. But why stop here? This work presents the analysis of the next challenge: a single-stage-to-orbit (SSTO) space tourism vehicle. Specifically, this work presents the parametric sizing (PS) analysis of a SSTO space tourism vehicle with a rocket-based combined-cycle (RBCC) engine and horizontal takeoff horizontal landing (HTHL) capabilities. This analysis was performed through the synthesis framework of hypersonic convergence. With hypersonic convergence, the wing planform area is iterated until the weight and volume budgets (functions of the structure, geometry, propulsion, mission, and system specifications) of the vehicle converge to define the takeoff gross weight. Consequently, the main results of this analysis were the 2-D and 3-D

solution space screenings of the takeoff gross weight versus planform area for an array of input variables, such as the slenderness parameter of the vehicle, and the comparison with other space tourism vehicle designs for sub-orbital and orbital missions.

TABLE OF CONTENTS

LIST OF ILLUSTRATIONS

LIST OF TABLES

CHAPTER 1

INTRODUCTION

1.1 Motivation

Ever since Yuri Gagarin became the first human to go to space in 1961 [1], there has been a never-ending and enduring interest in space and all its endless possibilities. In fact, a study performed by the think tank Pew Research Center in 2018 revealed that 72% of Americans believe it is essential that the United States continues to be a world leader in space exploration [2]. Individual ambition is indeed a reason why space exploration generates such an interest among all types of people [3]. However, it is the human curiosity, the desire to explore the unknown, the desire to discover new worlds, and every humans' "intangible desire to explore and challenge the boundaries of what we know and where we have been" [4] what really have been the driving force of space exploration all these decades [3,4]. As a consequence, what first started as a means of political rivalry has transformed into a collective effort that has resulted in the development of new technologies and industries in recent years. One of the new industries that have emerged and have developed significantly due to advances in space exploration is space tourism.

1.1.1 Introduction to Space Tourism

Space tourism can be defined as a branch of the aviation industry that has the mission of 1) giving tourists the opportunity of becoming astronauts without having to take all the required training and 2) making space travel a form of recreational, leisure, or business experience [5]. Or, simply explained, space tourism can be defined as the "flight

into outer space of humans for their own pleasure and excitement" [6]. Space tourism can be divided into three categories: short-duration sub-orbital flights, long-duration orbital flights, and flights beyond Earth's orbit (i.e., lunar and Mars flights) [5,7]. So far, the Russian Space Agency has been the only corporation to successfully provide space tourism through the form of orbital flights [7]. Engineer and entrepreneur Dennis Tito became the first-ever space tourist when he was taken in 2001 to the International Space Station (ISS) by the Russian Space Agency after paying $20 million for his flight [6]. Thereafter, the Russian Space Agency took six more tourists to the ISS at a flight price that was now as high as $35 million [7,8]. Unfortunately, due to space limitations in the ISS and limitations in launch mechanisms, the Russian Space Agency canceled all its space tourism flights in 2010 [7,8]. Fortunately, due to the significant improvement in technology in recent years, space tourism has resurfaced as a true possibility for the general public (to those who can afford it at least), only that this time it is being privately funded (i.e., no government support).

1.1.2 Space Tourism Today

Some of the aerospace companies that are privately funding and pursuing space tourism include Virgin Galactic, SpaceX, Blue Origin, Orion Span, and Boeing [7]. Not surprisingly, prominent figures in the aerospace industry have shared their support for space tourism. For example, the legendary American astronaut and engineer Buzz Aldrin has devoted his late years as an advocate on the US government to develop programs that would send civilians to the moon and, his broader dream, Mars, as he qualifies space tourism as the "logical outgrowth of the adventure tourist market" [9]. However, the arguably leading figure in the space tourism race is the founder of the Virgin Group,

Richard Branson. Virgin Galactic, founded in 2004 as a branch from the Virgin Group, has successfully developed a two-stage-to-sub-orbit (TSTSO) reusable launch system named the "SpaceShipTwo spaceflight system" [10,11]. This system consists of a carrier air-breathing engine aircraft (Scaled Composites WhightKnightTwo illustrated in Figure 1.1) that releases a hybrid rocket engine sub-orbital spaceplane (Scaled Composites SpaceShipTwo illustrated in Figure 1.2) at an altitude of 50,000 ft to reach space [10].

Figure 1.1: Scaled Composites WhiteKnightTwo [10]

Figure 1.2: Scaled Composites SpaceShipTwo [10]

As of May 2021, Virgin Galactic is attempting to become the first company to provide commercial sub-orbital space tourism by starting its flight program as early as the first quarter of 2022 after a series of unfortunate delays due to mechanical difficulties and the COVID-19 pandemic [10,12]. But why stop here? Or even more realistically, are we going to stop here?

1.2 Project Objectives

Aircraft and spacecraft design can be divided into three main phases: conceptual design, preliminary design, and detail design [13]. Thereafter, the conceptual design phase can be further divided into three steps: parametric sizing (PS), configuration layout (CL), and configuration evaluation (CE) [14,15]. Parametric sizing is a 1st order visualization of a vehicle's solution space for a given mission based on empirical data and reduced-order models [15]. This project focused on the analysis of the next challenge: a single-stage-to-orbit (SSTO) vehicle designed for space tourism. Specifically, the objective of this project was to perform a PS of a SSTO vehicle with a rocket-based combined-cycle (RBCC) engine (a combination of an air-breathing engine with a rocket engine), and horizontal takeoff horizontal landing (HTHL) capabilities. Or, in other words, the objective of this project was to analyze the possibility (and the respective implications) of a space access vehicle (SAV) that can take off from a runway and climb with an air-breathing engine (like traditional aircraft do) before switching to a rocket engine for a steeper and almost perpendicular ascent to reach space. Such analysis is important at this moment because once Virgin Galactic opens the door for sub-orbital space tourism, a new world of possibilities will open as well. This is true since as soon as humans find something they like, they want more of it, and they want it better. Putting this statement into the space

tourism context means that as soon as the lower limit of space is broken, a new goal or desire will appear. Questions like “How can we do it more efficiently?” or “What comes after the sub-orbital experience?” will begin to rise and consume people’s minds. Additionally, even though Virgin Galactic is at the vanguard of space tourism, the series of delays they have experienced (and even the crash of Virgin Space Ship (VSS) Unity due to human error on October 31, 2014 [11,16]) have paved the way for the rational inquiry if a better approach for space tourism is achievable and feasible. As a consequence, this project attempts to anticipate the future and provide solutions to all these inquiries by analyzing if an alternative propulsion system might enable the transition from sub-orbital to orbital space tourism and beyond. Hence, the main deliverables from this PS analysis were the solution space screening of the takeoff gross weight vs. planform area of the vehicle and the comparison with other space tourism vehicle designs.

1.3 Project Relationship to AVD1 and AVD2

To develop an appropriate understanding of the design process for space tourism vehicles based on their mission requirements and physical and economical limitations (such as aerodynamic and propulsion properties, trajectory constraints, weight constraints, stability and control constraints, manufacturing cost, operational cost, etc.), Aerospace Vehicle Design 1 (AVD1) consisted of reverse engineering Virgin Galactic’s TSTSO SpaceShipTwo system. The objective of this project was to engage in professional data-base (DB) and knowledge-base (KB) reference collection to build synthesis tools and develop an appropriate sizing methodology, respectively. The goal of the sizing methodology was to confirm the individual and combined system properties of the TSTSO system and to perform market, competition, technology, and benefit assessments.

Having developed the appropriate understanding of the design process for space tourism vehicles, Aerospace Vehicle Design 2 (AVD2) consisted of designing a single-stage to sub-orbit (SSTSO) HTHL rocket-powered vehicle for space tourism. With the foundation from the synthesis tools developed in AVD1, the objective of this project was to develop an appropriate PS methodology to identify the solution space topography for the vehicle, followed by the production of a feasible CL and a CE analysis. Similarly, market, competition, technology, and benefit assessments were performed to provide a comparison between the developed SSTSO and Virgin Galactic's TSTSO. Consequently, it was inferred that the focus of this project was to analyze and compare the implications, and requirements of a SSTO vehicle as to the possible next challenge of space tourism through a PS analysis and comparison. Overall, this project is meant to provide the strategic and logical sequence from the reverse engineering of a staging stratofly system in AVD1, to the design of a SSTSO HTHL vehicle in AVD2 to the PS analysis of a SSTO HTHL vehicle for space tourism applications.

1.4 History of the SSTO Concept

The concept of developing a reusable single-stage-to-orbit for any number of space-related applications is not something new. The concept of a SSTO reusable vehicle was first introduced by Phil Bono with his OOST (One-Stage Orbital Space Truck) and ROOST (R standing for reusable) systems in the late 1960s [17]. Shortly after, the Chrysler Corporation proposed their SSTO vehicle design called SERV (Single-Stage Earth-Orbital Reusable Vehicle) for the NASA Space Shuttle contract [17]. However, in an era where fully reusable vehicles were considered to be "expensive, difficult and probably not worth the effort" [17], NASA decided to go with the partially-reusable wing-body configuration

of the Space Shuttle Orbiter known by everyone today. Unfortunately (or rather fortunately for the strong advocates of the SSTO concept), even though the Space Shuttle was (and probably still is) the most state-of-the-art vehicle ever built, it presented a series of unforeseen setbacks. The Space Shuttle was meant to be a partially reusable, low-cost system Earth-to-orbit system [17]. However, the requirement for high-quality maintenance, manpower, and slight technical inefficiencies (such as using the same vehicle for carrying both light and heavy payloads) resulted in high operational costs and a not so reusable vehicle that would eventually lead to the end of the program in the early 2010s [17].

Exponential growth in technology and NASA's desire of reducing the operational cost of launching a payload to space, during and after the operational years of the Space Shuttle, has brought the concept of a SSTO reusable vehicle "back on the game" [18]. Generally speaking, SSTO vehicles can be classified based on their propulsion system (such as air-breathing, all rocket, combined cycle) and their takeoff/landing modality (such as horizontal takeoff horizontal landing, vertical takeoff vertical landing, and vertical takeoff horizontal landing). Notable SSTO vehicles such as the McDonell Douglas DC-X (all rocket with vertical takeoff vertical landing), the Lockheed Martin X-33 (all rocket with vertical takeoff horizontal landing), the Reaction Engines Skylon (combined cycle with horizontal takeoff horizontal landing), and the Rockwell X-30 also known as NASP or National Aero-Space Plane (airbreathing horizontal takeoff horizontal landing) have been proposed in the last three decades [19,20]. Yet, with the exception of Skylon that is currently under development, none of these vehicles (or any other proposed SSTO designs) were ever built, and their respective programs were canceled or transferred to different programs that were eventually canceled as well [17]. The main struggle with SSTO

vehicles has always been the high weight penalties that impact not only the operational cost but also the overall performance of the vehicle [20].

CHAPTER 2

LITERATURE REVIEW

2.1 Reference Collection

At this point, only the concepts of space tourism, single-stage-to-orbit vehicles, the project's objective, and its relationship with AVD1 and AVD2 have been introduced. However, the vital (and certainly required) technical information used to develop the parametric sizing analysis tools has not been introduced. References with the technical information pertinent to the aircraft/spacecraft parametric sizing analysis process were identified through a literature review process. The literature review process was crucial as it allowed the identification of technical information to not only develop the analysis methodology but also to corroborate the validity of the respective methodology results. Consequently, Table 2.1 on the following page contains all the applicable references that were collected during the literature review process.

The majority of the literature review references were identified through the American Institute of Aeronautics and Astronautics Aerospace Research Central (AIAA ARC) online database. The references consist mainly of conference papers, official reports, dissertations, and lecture materials. Finally, for a more logical sequence, the application of the literature review for developing the parametric sizing analysis methodology can be found in Chapter 3 of this report. On the other hand, the following subsection contains the elements and parametric characteristics that were identified and used for verification of the model.

Table 2.1: References for the Parametric Sizing Analysis

Ref.	Year	Author	Title
[21]	1980	Loftin	Subsonic Aircraft: Evolution and Matching of Size to Performance
[22]	1985	Roskam	Airplane Design Part I: Preliminary Sizing of Airplanes
[23]	1986	Cunningham	Thrust Vectoring for Single-Stage-to-Orbit, Horizontal Takeoff, Horizontal Landing, Space Vehicles
[24]	1996	Tomita	Feasibility Study of a Rocket-Powered HTHL-SSTO with Ekranoplane as Takeoff Assist
[25]	2000	Curran	Scramjet Propulsion
[26]	2003	Crocker	A Comparison of Horizontal Takeoff RLVs for Next Generation Space Transportation
[27]	2004	Dissel	Comparison of HTHL and VTHL Air-Breathing and Rocket Systems for Access to Space
[28]	2006	Froning	Single-Stage HTHL Spaceplane Requirements for Orbital and Sub-Orbital Hypersonic Space Tourism Flight
[29]	2009	Nakane	Feasibility Study on Single Stage to Orbit Space Plane with RBCC Engine
[15]	2010	Coleman	Aircraft Conceptual Design – An Adaptable Parametric Sizing Methodology
[13]	2010	Nicolai	Fundamentals of Aircraft and Airship Design
[19]	2011	Longstaff	The SKYLON Project
[30]	2012	Chudoba	Solution-Space Screening of a Hypersonic Endurance Demonstrator
[31]	2014	Hempsell	SKYLON Users' Manual
[32]	2014	Gong	Design and Optimization of RBCC Powered Suborbital Reusable Launch Vehicle
[33]	2015	Mehta	Skylon Aerodynamics and SABRE Plumes
[34]	2018	Raymer	Aircraft Design: A Conceptual Approach
[35]	2018	Czysz	Future Spacecraft Propulsion Systems and Integration Enabling Technologies for Space Exploration
[36]	2020	Maynard	Hypersonic Convergence Background and Methodology
[37]	2020	Ferretto	Innovative Multiple Matching Charts Approach to Support the Conceptual Design of Hypersonic Vehicles
[38]	2020	Hassan	Design Tools for Conceptual Analysis of Future Commercial Supersonic Aircraft

2.2 Technical Data for Methodology Verification

As previously mentioned, the literature review process was also used to collect data references for verification of the model. As of May 2021, although multiple concept papers discussing the current technological feasibility for a SSTO vehicle have been published, not a single SSTO space access vehicle with a RBCC engine and HTHL capabilities has ever been built. However, as mentioned in the introduction, there is one SSTO vehicle with

a RBCC engine and HTHL capabilities currently under development: Reaction Engine's Skylon spaceplane [19,33]. The origins of Skylon dates around the early 1980s when British engineers Alan Bond and Bob Parkinson envisioned the transition from expendable launch vehicles (ELVs) to reusable launch vehicles (RLVs) [19]. Additionally, with their technological and cost assessment, Bond and Parkinson concluded that a SSTO vehicle rather than a multi-stage would be more cost-efficient in the long run [19]. Skylon's design has varied numerously throughout the years. The latest design, and the one being currently under development, is Configuration D1 shown in Figure 2.1 and Figure 2.2 below.

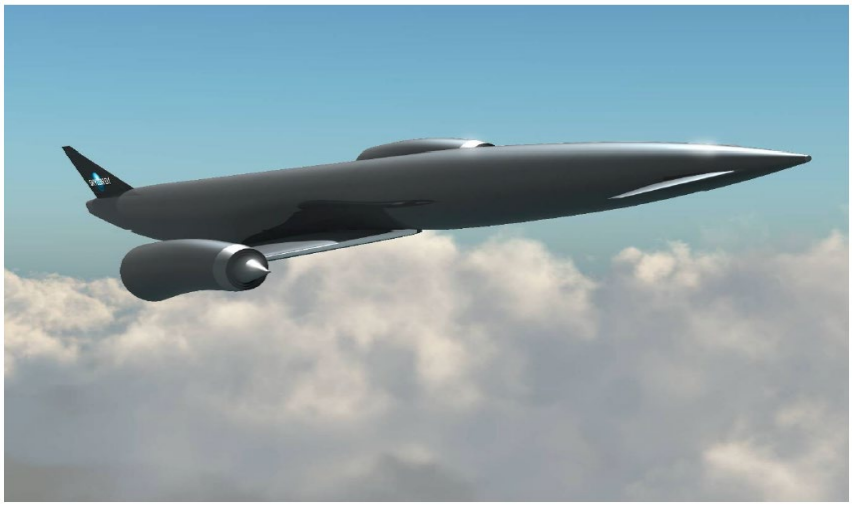

Figure 2.1: Artistic Rendering for Skylon (Configuration D1) [31]

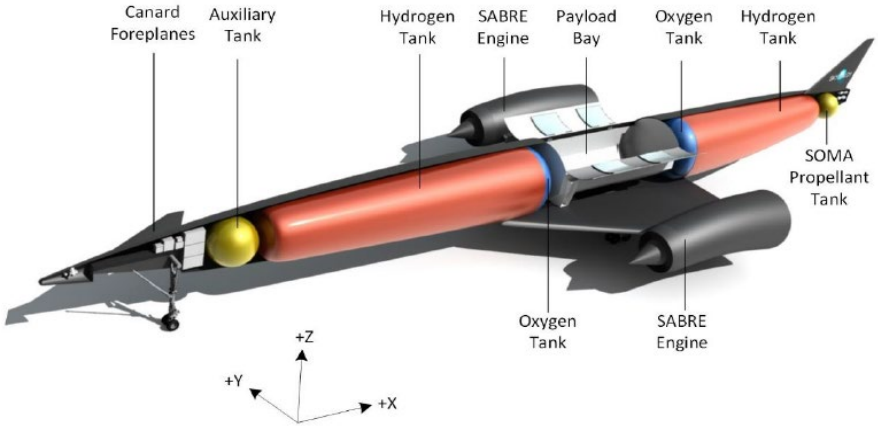

Figure 2.2: Skylon Layout [31]

The current Skylon configuration consists of 4 Synergetic Air-breathing Rocket Engines (SABRE) [19,31,33]. These revolutionary engines are capable of pre-cooling the freestream air before compressing it at high pressures so that it can be stored and used as an oxidizer for Skylon's state-of-the-art liquid hydrogen/liquid oxygen rocket engine [31]. Additionally, the efficiency of the system is further increased as the heat extracted from the air during compression is used as an energy source to power the compressor itself and the fuel pumps [31]. As a consequence, Skylon is capable of increasing the mass ratio for almost twice the value of an all-rocket engine that has an equal efficiency [31,33]. The SABRE engine is designed to accelerate from Mach 0 to Mach 5.5 in a 28 km climb from sea level, before switching to the rocket engine that accelerates from Mach 5.2 to Mach 27.8 at an altitude range between 28 and 90 km [31]. Finally, if optimized for space tourism, Skylon is capable of carrying up to 24 passengers and a captain to orbit. A summary of Skylon's weight distribution is illustrated in Table 2.2 below. From this table, it can be seen that the theoretical TOGW for Skylon is 325 metric tons or 325,000 kg. Finally, using Eq. (2.1) also below, the calculated fuel fraction of the vehicle was determined to be 0.7695.

Table 2.2: Skylon's Mass Distribution [31]

Item	Mass Contribution (Metric Tons)
Dry Vehicle	53.5
Consumables	6.5
Usable Ascent Propellant	250.1
Nominal Payload	15.0
Takeoff Gross Weight (TOGW)	325.0

$$ff = \frac{w_{fuel}}{TOGW} = \frac{250.1\ tons}{325\ tons} = 0.7695 \tag{2.1}$$

Up until this moment, only half of the parameters that are required for the verification of the solution space model have been identified; the only missing verification parameter is the theoretical planform area for Skylon. Unfortunately, none of the literature review references provided an estimation of the planform area. Consequently, an "out of the box" solution was required. Upon further research in online engineering data libraries and tools, an OpenVSP model of the Skylon Configuration D1 was identified. OpenVSP is a "parametric aircraft geometry tool" that can be used to create 3-D models of various aircraft for engineering analysis [39]. This specific model was scaled down and developed based on the geometrical dimensions of Skylon that are shown in Ref. [31]. Figure 2.3 below includes the isometric projection and top view of Skylon from the OpenVSP model.

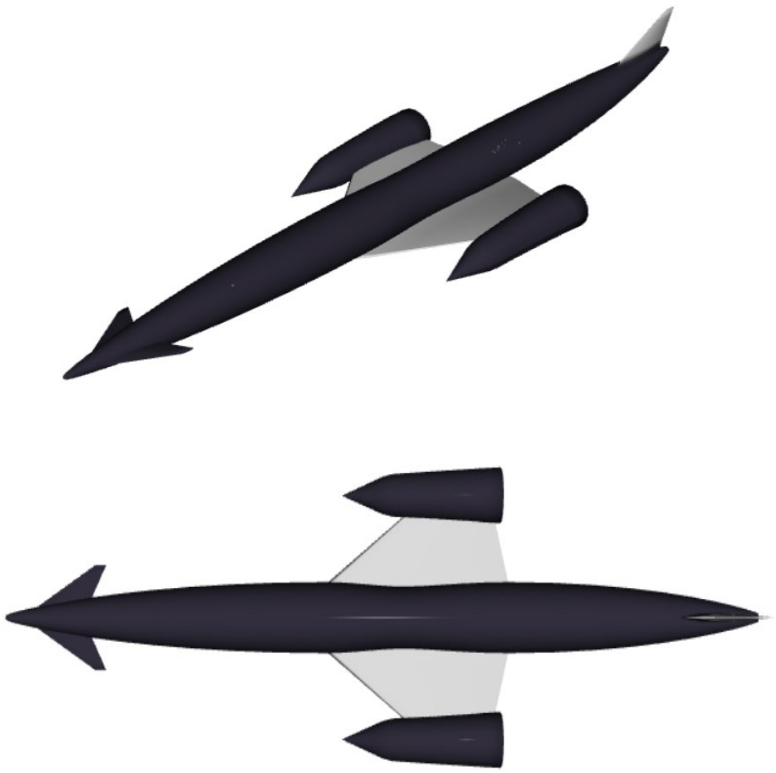

Figure 2.3: OpenVSP Model of Skylon [40]

Finally, a geometrical analysis of the OpenVSP model was performed with Jenor Rasmussen, a fellow senior aerospace engineer. The geometrical analysis (shown in Figure 2.4) indicated that the theoretical planform area for Skylon has a value of 353.39310 m^2.

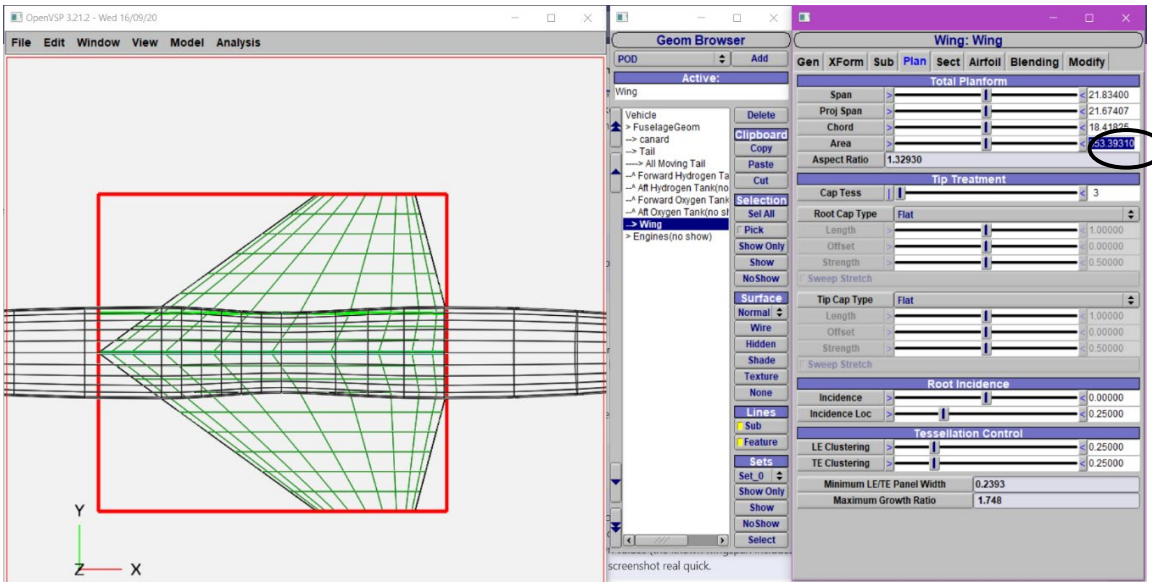

Figure 2.4: Geometrical Analysis of the Skylon OpenVSP Model

A summary of the main verification values for the parametric sizing methodology is illustrated in Table 2.3 below.

Table 2.3: Summary of the Verification Values for the PS Model

Parameter	Dimension
Takeoff Gross Weight (TOGW)	325,000 kg
Planform Area (S_{pln})	353.39310 m^2
Fuel Fraction (ff)	0.7695

CHAPTER 3

METHODOLOGY

3.1 Traditional Sizing Methodologies

Throughout the years, multiple methodologies have been developed to perform the PS analysis of an aircraft or spacecraft during the conceptual design phase. Some of the most prominent methodologies include the ones developed by Nicolai [13], Coleman [15], Loftin [21], Roskam [22], and Raymer [34]. For instance, Roskam's methodology starts by allowing the user to assume or guess an initial TOGW [22,36] followed by the identification of the empty weight (W_E) from empirical correlations [36]. Thereafter, the fuel weight (W_F) is determined from trajectory estimations based on the Breguet range equations for climb and cruise conditions after having assumed fuel fractions for taxi, takeoff, descent, and landing, as well as a lift to drag ratio (L/D) and specific fuel consumption (SFC), from standard industry values [36]. From these weight parameters, performance constraints such as the wing loading (i.e., the weight of the vehicle over the wing area, W/S) for stall and landing, and the thrust to weight ratios (T/W) for the takeoff, climb, and cruise phases are developed to determine the feasible solution space of the vehicle as shown in Figure 3.1 on the following page [36]. From this solution space, the wing planform area, the required thrust, and a new TOGW can be determined. This process is then repeated by iterating the TOGW until the old TOGW and the new TOGW converge below a specified tolerance to conclude the sizing of the vehicle [36]. Roskam's parametric sizing methodology is summarized in Figure 3.2 also on the following page together with

the design methodologies derived by Nicolai and Loftin.

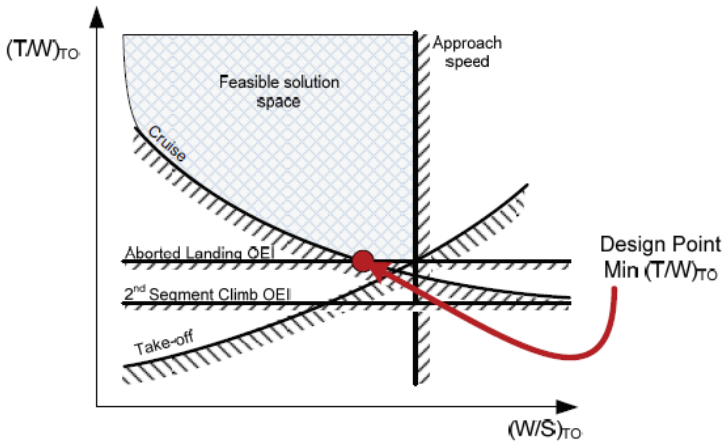

Figure 3.1: Classical Solution Space Screening [15]

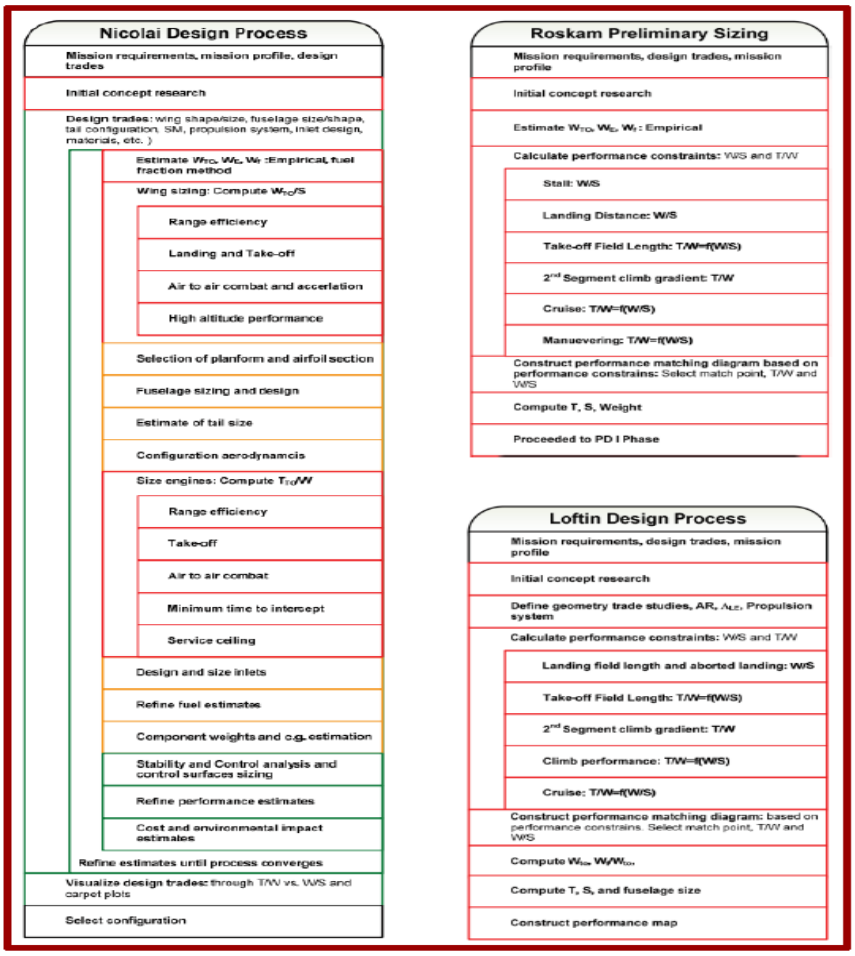

Figure 3.2: Summary of the Parametric Sizing Methodologies Developed by Nicolai, Roskam, and Loftin [36]

Unfortunately, for the purposes of the parametric sizing analysis of a SSTO vehicle, these traditional sizing methodologies present a significant problem. The problem is that these methodologies were mainly derived for subsonic (a flight Mach number less than 1) and supersonic (a flight Mach number greater than 1 but less than 5) vehicles [36]. As a consequence, only the wing and the propulsion system are sized together, allowing the fuselage and the empennage of the vehicle to be sized independently [36]. The sizing methodology of a hypersonic vehicle (a vehicle with a flight Mach number greater than 5), such as a SSTO vehicle susceptible to experience high Mach numbers during powered ascent and/or atmospheric reentry, "must consider the total integration of the system simultaneously" as changes to one parameter result in changes to other dependent parameters as shown in Figure 3.3 [36]. As the flight velocity increases substantially, changes to optimize an individual parameter will lead to non-optimum changes in other parameters that will either need to be fixed (resulting in a never-ending cycle of changes) or will result in a non-optimum design [36]. Both of these scenarios are unacceptable, and, as a consequence, an alternative methodology had to be developed and employed.

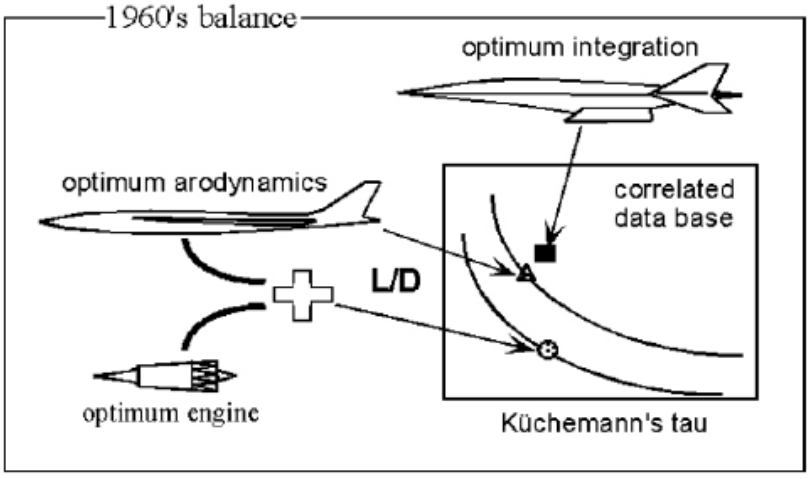

Figure 3.3: Correlation of an Optimal Integrated Vehicle vs a Vehicle with Independently Sized Optimal Components [36]

3.2 Hypersonic Convergence

3.2.1 Sizing Logic

The solution to the non-optimal sizing dilemma previously discussed came through the implementation of the hypersonic convergence methodology. The hypersonic convergence methodology operates by explicitly including the vehicle's volume into the convergence logic to integrate the fuselage, aerodynamic surfaces, and the propulsion system simultaneously [15,30]. At its core, what hypersonic convergence does is that it iterates the wing planform area of the vehicle until the weight and volume budgets converge to define the TOGW for a given mission [36]. The weight and volume budgets are defined as functions of the structure, geometry, propulsion, mission, and system specifications of the vehicle, and they can be mathematically illustrated as shown in Eq. (3.1) and Eq. (3.2) below. Mathematical convergence in hypersonic convergence occurs once both sides of Eq. (3.3) are found to be equal.

$$W_{OEW} = \frac{I_{str}K_W S_{pln} + C_{sys} + \frac{(T/W)_{max}W_R}{E_{TW}}\left(W_{pay} + W_{crew}\right) + W_{cprv}}{\frac{1}{1+\mu_a} - f_{sys} - \frac{(T/W)_{max}W_R}{E_{TW}}} \tag{3.1}$$

$$W_{OWE} = \frac{\tau S_{pln}^{1.5}(1 - k_v - k_{vs}) - v_{fix} - N_{crw}(v_{crw} - k_{crew}) - W_{pay}/\rho_{pay}}{\frac{WR - 1}{\rho_{ppl}} + (k_{ve}(T/W)_{max}W_R)} \tag{3.2}$$

$$W_{OWE} = W_{OEW} + W_{pay} + W_{crew} \tag{3.3}$$

Thereafter, the iteration process is repeated for an array of inputs such as τ, the slenderness parameter of the vehicle, or the payload mass to generate the solution space screening, which resembles a "carpet plot consisting of the converged plots" [36]. In most

cases, τ is usually selected as the input variable, as it enables the analysis of the geometric slenderness to determine the lowest vehicle weight that will still be able to meet the mission requirements [36]. Finally, the hypersonic convergence methodology is summarized in Figure 3.4 shown below.

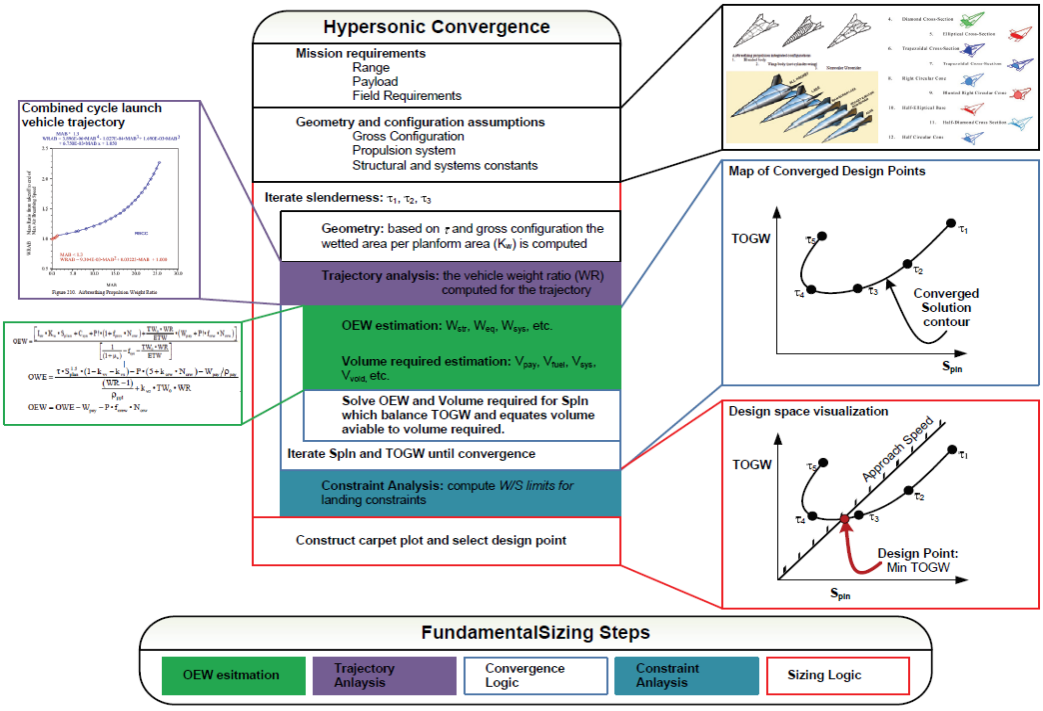

Figure 3.4: Summary of the Hypersonic Convergence Methodology [15]

3.2.2 Variables and Constants in the Weight and Volume Budget Equations

As it is evident from Eq. (3.1) and Eq. (3.2), the weight and volume budgets for a given vehicle are dependent on multiple parameters from other disciplines. These parameters can be either constant or variable, depending on the way that they are being defined by the user. The equations needed to define the variable parameters during hypersonic convergence were identified from Paul Czysz's paper in Scramjet Propulsion [25] and from Ian Maynard's hypersonic convergence lecture [36]. The equations for the variable parameters in the weight budget are illustrated from Eq. (3.4) to Eq. (3.11) while

the equations for the variable parameters in the weight budget are illustrated from Eq. (3.12) to Eq. (3.17).

$$W_{str} = I_{str} \cdot K_w \cdot S_{pln} = I_{str} \cdot S_{wet} \tag{3.4}$$

$$C_{sys} = C_{un} + f_{mnd} \cdot N_{crw} \tag{3.5}$$

$$W_{sys} = C_{sys} + f_{sys} \cdot W_{dry} \tag{3.6}$$

$$W_{eng} = \frac{TW_0 \cdot WR}{ETW} \cdot OWE \tag{3.7}$$

$$W_{cprv} = f_{cprv} \cdot N_{crw} \tag{3.8}$$

$$W_{crw} = f_{crw} \cdot N_{crw} \tag{3.9}$$

$$W_{dry} = (1 + \mu_a)\left(W_{str} + W_{eng} + W_{sys} + W_{cprv}\right) = OWE \tag{3.10}$$

$$WR = \frac{1}{1 - ff} \tag{3.11}$$

$$V_{ppl} = \frac{OWE \cdot (WR - 1)}{\rho_{ppl}} \tag{3.12}$$

$$V_{fix} = V_{un} + f_{crw} N_{crw} \tag{3.13}$$

$$V_{sys} = V_{fix} + k_{vs} \cdot V_{tot} \tag{3.14}$$

$$V_{void} = k_{vv} V_{tot} \tag{3.15}$$

$$V_{pay} = \frac{W_{pay}}{\rho_{pay}} \tag{3.16}$$

$$V_{crw} = \left(V_{pcrw} + k_{crw} \cdot N_{crw}\right) \tag{3.17}$$

Moving on, some of the variables needed in the previous equations can be defined as constants based on historical values as well as current and future industrial capabilities. Hence, Table 3.1 lists the range of the constant parameters for the weight budget equation while Table 3.2 lists the range of the constant parameters for the volume budget equation.

Table 3.1: Range of Constant Parameters for the Weight Budget [25,36]

Variable Name	Symbol	Range	Units
Structural Index	I_{str}	$17 \leq I_{str} \leq 21$	kg/m^2
System Weight Coefficient	f_{sys}	$0.16 \leq f_{sys} \leq 0.24$	ton/ton
Unmanned System Weight	C_{un}	$1.9 \leq C_{un} \leq 2.1$	ton
Crew System Weight	f_{mnd}	$1.45 \leq f_{mnd} \leq 1.05$	ton
Engine Thrust to Weight Ratio	E_{TW}	$10 \leq E_{TW} \leq 25$	$kg\ thrust/kg\ weight$
Provisions to Accommodate Crew	f_{cprv}	$0.45 \leq f_{cprv} \leq 0.50$	$ton/person$
Crew Member Specific Weight	f_{crw}	$0.14 \leq f_{crw} \leq 0.5$	$ton/person$

Table 3.2: Range of Constant Parameters for the Volume Budget [25,36]

Variable	Symbol	Range	Units
Unmanned System Volume	V_{un}	$5.0 \leq V_{un} \leq 7.0$	m^3
Crew Member Volume	f_{crw}	$11 \leq f_{crw} \leq 12$	$m^3/person$
System Volume Coefficient	k_{vs}	$0.02 \leq k_{vs} \leq 0.04$	m^3/m^3
Engine Volume Coefficient	k_{ve}	$0.25 \leq k_{ve} \leq 0.75$	$m^3/ton\ thrust$
Void Volume Coefficient	k_{vv}	$0.10 \leq k_{vv} \leq 0.20$	m^3/m^3
Payload Density	ρ_{pay}	$48 \leq \rho_{pay} \leq 130$	kg/m^3
Crew Member Volume	k_{crw}	$0.9 \leq k_{crw} \leq 2.0$	$m^3/person$
Crew Provisions Volume	V_{pcrw}	$6 \leq k_{crw} \leq 5$	$m^3/person$

It was previously mentioned that the traditional input variable to generate the solution space in hypersonic convergence is τ, Küchemann's slenderness parameter. In hypersonic convergence, τ is a non-dimensional parameter that relates the volume of the vehicle to the wing planform area and serves the same function that the wing loading (W/S) does in the traditional parametric sizing approaches previously introduced [15,36]. The

main difference to the wing loading is that τ relates the wing planform area to the volume rather than to the weight of the vehicle to deliver a simultaneous sizing of not only the wing loading and the weight but also the volume of the vehicle [15]. As τ increases for a given configuration, the vehicle possesses more volume per unit planform area, making its geometry stouter [15]. On the other hand, as τ decreases, the vehicle becomes more slender [15]. This behavior can be visually appreciated with Figure 3.5 shown below.

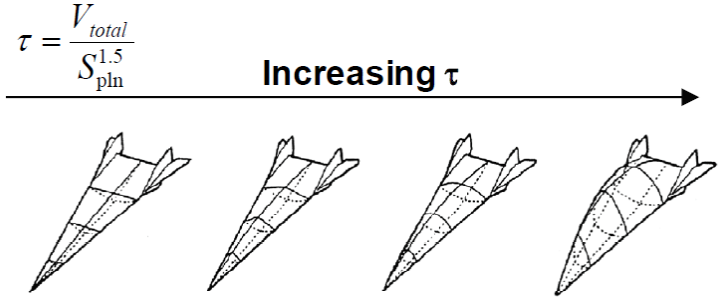

Figure 3.5: Explanation of the Effect of $\boldsymbol{\tau}$ in the Volume of a Vehicle [15]

For a given analysis, the range of τ for the hypersonic convergence model will depend on the range of the morphing geometry of interest, and the selected τ will define the final geometry of the vehicle [36]. The morphing geometry of a vehicle is a function of τ and K_w (the ratio of the wetted area to the planform area), which is already a function of τ [36]. Figure 3.6 on the following page presents a plot of K_W vs τ superimposed with what the vehicle geometry and propulsion system are expected to be for a given K_w and τ combination at a $72°$ sweep angle (one exception applied). Skylon, the vehicle used for verification of the model and previously introduced in Chapter 2, can be considered as a wing-body geometry or maybe even a cylinder wing. Consequently, the results from the hypersonic convergence analysis should indicate a τ value between 0.10 and 0.21.

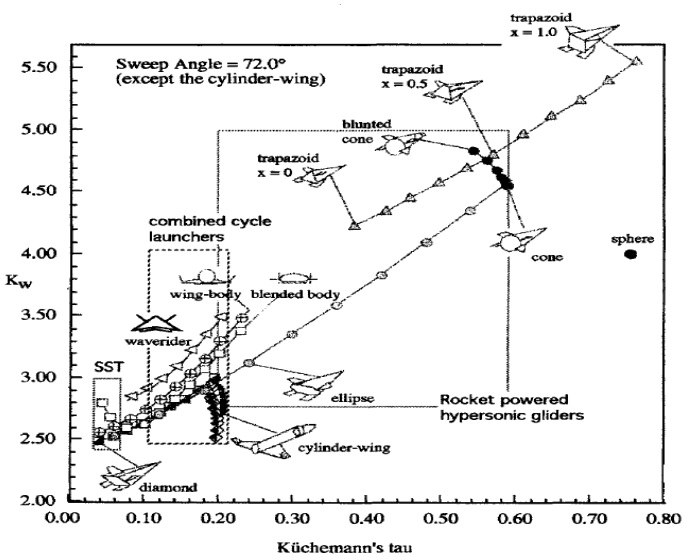

Figure 3.6: Geometrical Configuration of Hypersonic Vehicles as a function of $\boldsymbol{\tau}$ [25]

Finally, K_w as a function of τ can be generically defined as shown in Eq. (3.18) below. This definition was derived based on the overall mission of the vehicle without any specific geometrical considerations [25]. However, specific K_w equations for a given geometry of interest can also be employed for hypersonic convergence [15,36,41].

$$\frac{K_w}{\tau} = \exp(0.081[\ln \tau]^2 - 0.0461 \ln \tau + 1.738) \tag{3.18}$$

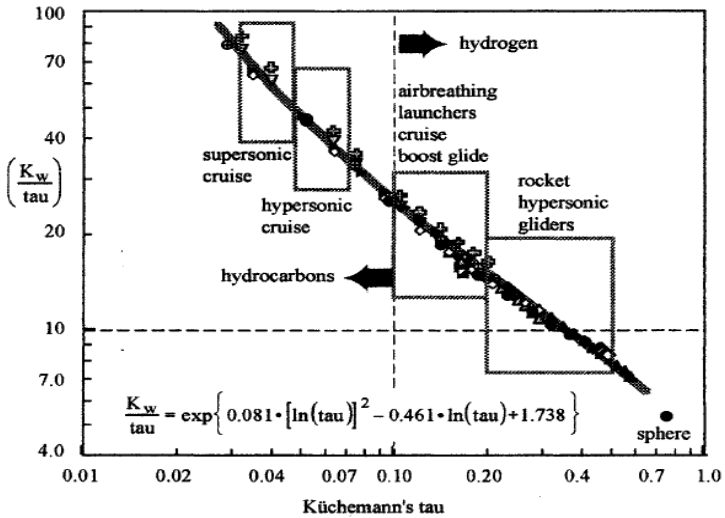

Figure 3.7: $\boldsymbol{K_w}$ as a function of $\boldsymbol{\tau}$ based on Mission Specifications [25]

CHAPTER 4

DISCUSSION

4.1 Model Verification

Having derived the appropriate methodology for the PS analysis, the next step was to develop the computerized hypersonic convergence model through the MATLAB interface and verify the accuracy of the results. To do so, however, all the constant variables for the analysis had to first be defined. As a consequence, the values for the constant parameters in the weight budget equation were determined from their respective range in Table 3.1, and they are shown in Table 4.1 below. Similarly, the values for the constant parameters in the volume budget equation were determined from their respective range in Table 3.2, and they are shown in Table 4.2 on the following page. These values were selected based on current industrial capacities and traditional values for a wing-body geometry configuration (both found in *Scramjet Propulsion* [25]), as it was assumed that Skylon possesses a wing-body geometry and its respective properties.

Table 4.1: Chosen Values for the Constant Parameters in the Weight Budget Equation

Parameter	Numerical Value	Units
I_{str}	21	kg/m^2
f_{sys}	0.16	ton/ton
C_{un}	2.1	ton
f_{mnd}	1.05	ton
E_{TW}	13.2857	$kg\ thrust/kg\ weight$
f_{cprv}	0.50	$ton/person$
f_{crw}	0.15	$ton/person$

Table 4.2: Chosen Values for the Constant Parameters in the Volume Budget Equation

Parameter	Numerical Value	Units
V_{un}	7.0	m^3
f_{crw}	12	$m^3/person$
k_{vs}	0.04	m^3/m^3
k_{ve}	0.40	$m^3/ton\ thrust$
k_{vv}	0.15	m^3/m^3
ρ_{pay}	130	kg/m^3
k_{crw}	2.0	$m^3/person$
V_{pcrw}	5.0	$m^3/person$

Thereafter, it was necessary to specify the weight ratio (WR) as a function of the mission and/or trajectory specifications of the vehicle. As previously mentioned in Chapter 2, Skylon is being designed to accelerate with an air-breathing engine from Mach 0 to Mach 5.5 from sea level to an altitude of 28 km, before switching to a rocket engine that accelerates from Mach 5.2 to Mach 27.8 between 28 and 90 km [31]. Consequently, the weight ratio for both phases can be determined and multiplied together to calculate the total weight ratio of the vehicle. The weight ratio for each phase can be defined as shown in Eq. (4.1) below where ΔV is the difference between the final velocity and the initial velocity, g_0 is the acceleration due to gravity at sea level, and I_{sp} is the specific impulse, a propulsion characteristic of the vehicle engine.

$$WR = \exp\left(\frac{\Delta V}{g_0 I_{sp}}\right) = \exp\left(\frac{V_f - V_i}{g_0 I_{sp}}\right) \tag{4.1}$$

Reaction Engines indicates in the Skylon user manual that the approximate specific impulse during the air-breathing ascent is between 40000 $N \cdot s/kg$ and 90000 $N \cdot s/kg$ [31]. Similarly, the approximate specific impulse during the rocket ascent is indicated to be 4500 $N \cdot s/kg$ [31]. Thereafter, the velocity at a given altitude can be defined as the

product of the Mach number (M) and the speed of sound (a) at the given altitude, as shown in Eq. (4.2) below.

$$V = M * a \tag{4.2}$$

In a similar manner, the speed of sound can be defined as a function of the temperature T at a given altitude as shown in Eq. (4.3) below, where γ is the ratio of specific heats, and R is the specific gas constant of air. Finally, the temperature at each altitude can be determined using the standard atmosphere model equations that were empirically derived and are shown in Ref. [42]. Using the indicated Mach number and altitude transition combinations, and a specific impulse of 50000 $N \cdot s/kg$ for the air-breathing engine, the weight ratios for the air-breathing engine and rocket engine were identified to be 1.0336 and 3.6675, respectively. Consequently, the weight ratio for the total vehicle was determined to be 3.7907.

$$a = \sqrt{\gamma RT} \tag{4.3}$$

Moving on, the propellant density (ρ_{ppl}) needed for the volume budget equation can be identified from the propulsion specification of the vehicle's engine. The SABRE engine used by Skylon uses liquid hydrogen (LH_2) as fuel and liquid oxygen (LOX) as oxidizer [31,33]. Consequently, the fuel density (ρ_{fuel}) and oxidizer density ($\rho_{oxidizer}$) were identified to be 71 kg/m^3 and 1141 kg/m^3 respectively [43]. Then, by assuming an optimal oxidizer to fuel ratio ($r_{O/F}$) of 6, the propellant density was determined to be 361.887 kg/m^3 using Eq. (4.4) shown below.

$$\rho_{ppl} = \frac{\rho_{fuel}\left(1 + r_{O/F}\right)}{1 + r_{O/F} + \frac{\rho_{fuel}}{\rho_{oxidizer}}} \tag{4.4}$$

Finally, a nominal number of 20 passengers (i.e., payload) and one crew member were selected for verification [31]. Additionally, the margin of inert weight (μ_a) was selected to be 15% [25]. With all constant parameters being known, the hypersonic model was developed, and it resulted in the TOGW vs S_{pln} curve illustrated in Figure. 4.1 shown below.

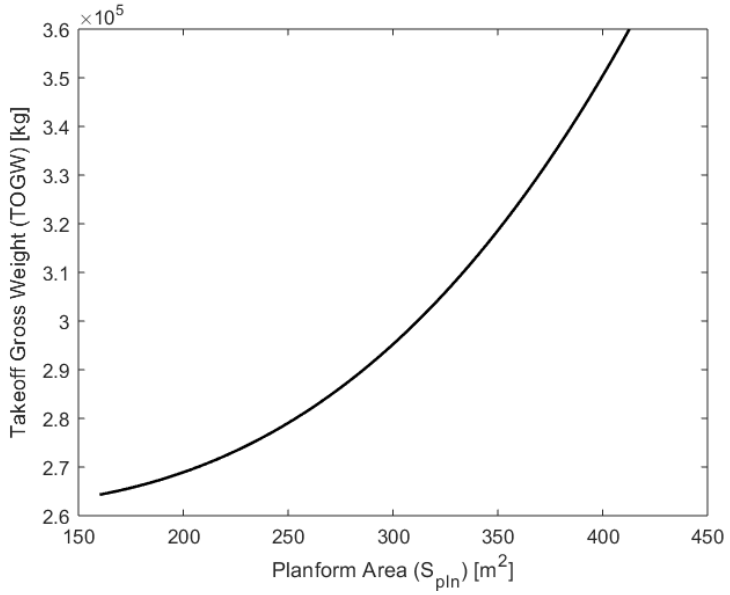

Figure 4.1: Raw Solution from the Hypersonic Convergence Model

As previously mentioned, design constraints must be added to do the hypersonic convergence solution to fully develop the solution space and identify the feasible design solutions [36]. For simplicity, only the takeoff wing loading constraint was considered for this analysis. The takeoff wing loading, $(W/S)_{TO}$, can be defined as shown in Eq. (4.5) below where ρ is the density of air, V_{TO} is the takeoff velocity, and $C_{L,TO}$ is the lift coefficient during takeoff.

$$(W/S)_{TO} = 0.5\rho V_{TO}^2 C_{L,TO} \tag{4.5}$$

First, based on the Mach number and altitude schedule previously introduced, the takeoff altitude was determined to be at sea level, resulting in an air density of $1.225\ kg/m^3$. From the Skylon user's manual, the takeoff velocity was identified to be 155 m/s [31]. The identified takeoff velocity resulted in a Mach number of 0.4555, which falls within the range of acceptable Mach numbers that SSTO HTHL vehicles can experience during takeoff [19,24]. Thereafter, the traditional range for the takeoff lift coefficient of a wing-body geometry vehicle was identified to be between 0.4–0.8 [44]. Hence, an average takeoff lift coefficient of 0.6 was used for the analysis. Finally, multiplying the takeoff wing loading with the range of feasible planform areas from Figure 4.1 and dividing by gravity to match units, the wing loading constraint was identified. Consequently, the wing loading constraint was incorporated into the hypersonic convergence model solution to develop the solution space as shown in Figure 4.2 below. In this figure, the intersection of the two curves denotes the design point of the vehicle.

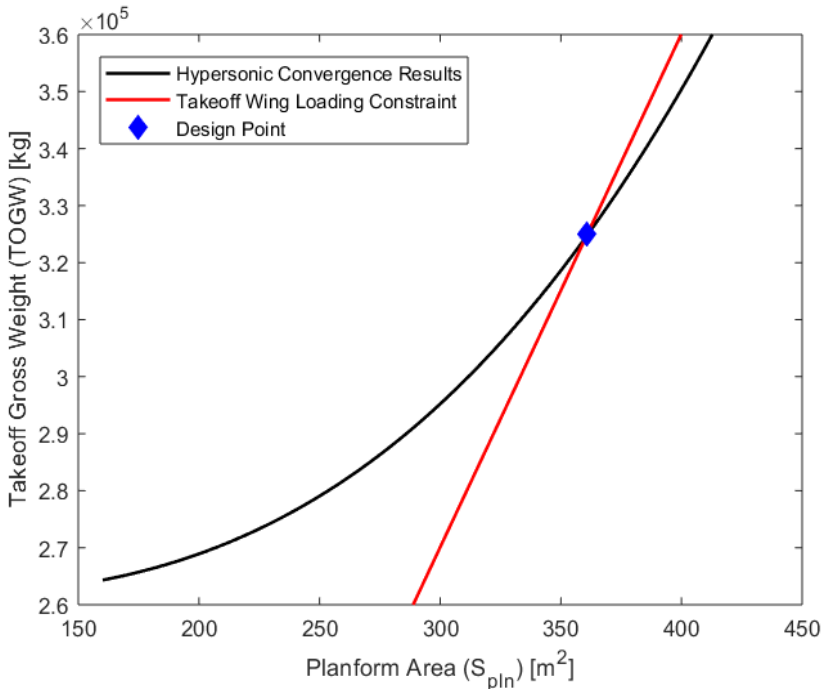

Figure 4.2: Generated Solution Space for the Skylon Spaceplane

From Figure 4.2, the design point of Skylon was identified to be a TOGW of 325,000 kg and a planform area of 361 m^2. The calculated design point conditions were compared to the theoretical values as shown in Table.4.3 below. This comparison indicated that the model results were within a 5% error margin, allowing the conclusion that the developed model is accurate, correct, and precise. Additionally, the Küchemann's slenderness parameter of the vehicle was identified to be 0.1725, falling within the range of expected values that were introduced in Chapter 3.

Table 4.3: Comparison of the Theoretical and Calculated Parameters for Skylon

Parameter	Theoretical	Calculated	Percent Error
TOGW	325,000 kg	325,000 kg	0%
Planform Area	353.39310 m^2	361 m^2	1.96%
Fuel Fraction	0.7695	0.7362	4.42%

4.2 Sizing Comparison with Other Space Tourism Vehicles

Having verified the accuracy of the developed methodology and mathematical model for a single mission requirement, it was then possible to increase the range of mission requirements for a better comparison with other space tourism vehicle designs. In other words, as the main objective of space tourism is to carry people to space, the weight of the payload (i.e., the number of passengers) was varied to understand its effect on the vehicle size. The takeoff wing loading design constraint and other vehicle properties such as the geometry (wing-body), propulsion (SABRE engine with LH_2/LOX propellant), weight and volume budget constant parameters, and trajectory specifications were kept unaltered. By varying the Küchemann's slenderness parameter of the vehicle and the payload weight, a 3-D solution space was generated, and it is illustrated in Figure 4.3 on the following page. Similarly, Figure 4.4 and Figure 4.5 present the solution spaces that were generated for SpaceShipTwo (Virgin Galactic's TSTSO system) in AVD1 and

Aspiration, the proposed SSTSO, lifting-body, all-rocket vehicle that was designed in AVD2.

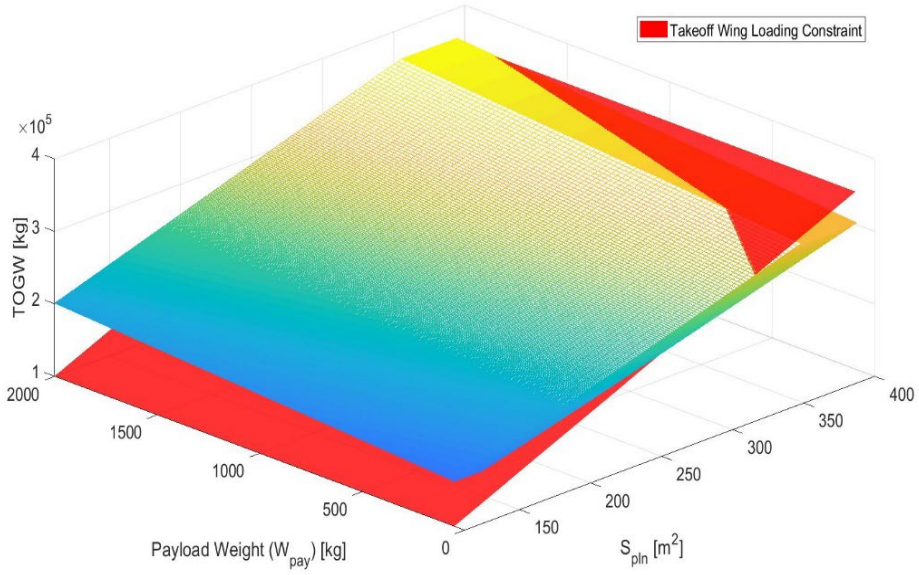

Figure 4.3: Solution Space of a SSTO Vehicle with a RBCC Engine

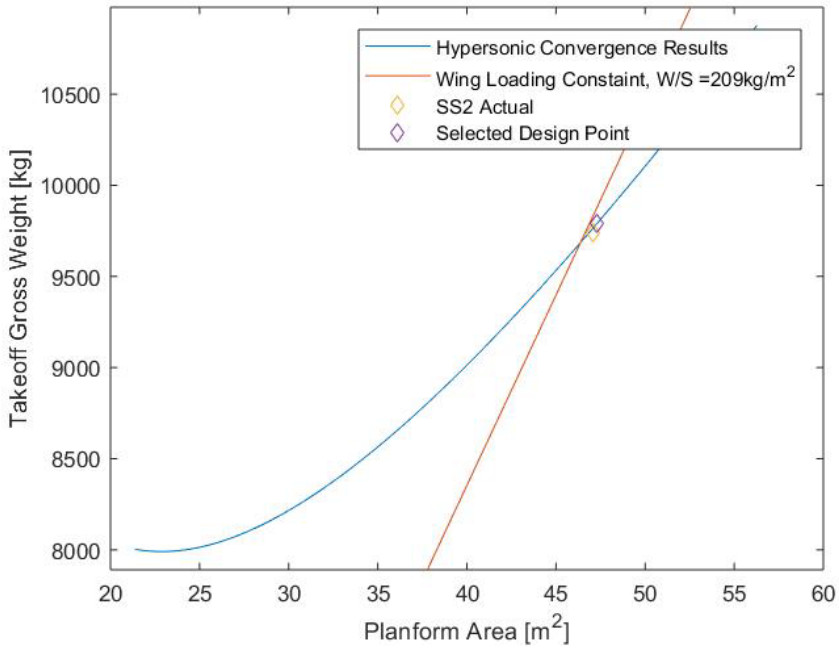

Figure 4.4: Solution Space of SS2: TSTSO Vehicle [45]

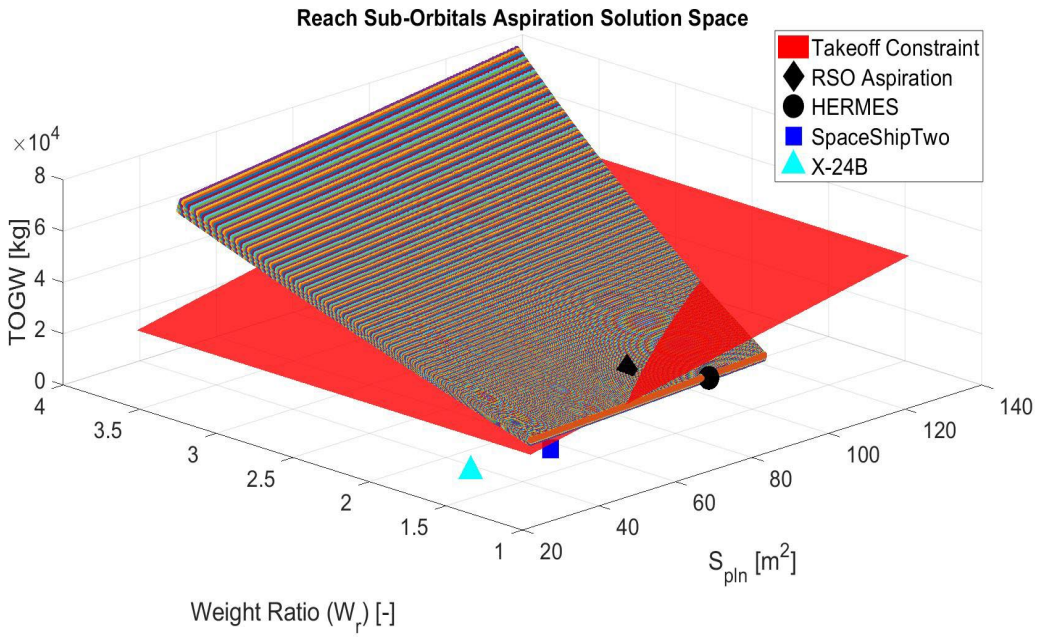

Figure 4.5: Solution Space of Aspiration: SSTSO All-Rocket Vehicle [46]

Important conclusions can be made by comparing all the solution spaces from Figure 4.3 to Figure 4.5. Starting with the sub-orbital vehicles (SpaceShipTwo in Figure 4.4 and Aspiration in Figure 4.5), at first sight, it seems to appear that the SSTSO vehicle requires a much higher TOGW (23,221 kg) than the TSTSO vehicle (9740 kg) for the given mission. However, this comparison is not entirely accurate if the TOGW of the first stage of SpaceShipTwo (i.e., WhiteKnightTwo) is not considered. WhiteKnightTwo possesses a TOGW of about 31,751 kg (70,000 lb) [16]. Consequently, the true TOGW for the TSTSO system must be the addition of SpaceShipTwo and WhiteKnightTwo, resulting in a total TOGW of 41,491 kg. Comparing this value with the TOGW of the SSTSO indicates that it is now the SSTSO system, the one with the smallest TOGW. This conclusion gives Aspiration an advantage over the SpaceShipTwo and WhiteKnightTwo system since a higher TOGW would require a greater thrust generation, which would require more engines or bigger engines, which would then require more fuel, resulting in a higher operational

cost. In a market as uncertain as space tourism, such additional charges must be avoided at all costs. It must be remarked that the TOGW comparison is not highly affected by the fact that one vehicle possesses a lifting body geometry (to be explained later) while the other possesses a traditional wing-body configuration.

Moving on, the solution spaces for these two systems also enable the comparison of the required planform areas for the given mission. Figure 4.4 and Figure 4.5 indicate that a higher planform area is required for the SSTSO vehicle (74 m^2) than for the TSTSO vehicle (47 m^2). This conclusion is easily explained by analyzing the wing loading of the vehicle. For simplification, it can be assumed that the critical moment in the mission profile for which the wing of the space tourism vehicle must be sized is the pull up maneuver for the powered ascent. Then, as the wing loading of the vehicle decreases during the pull-up, the performance of the pull-up maneuver increases as more lift is generated for a given amount of thrust. The wing planform area of SpaceShipTwo was sized to assure such a maneuver at a given thrust and a given TOGW. On the other hand, the weight of Aspiration during pull-up is not the TOGW (as fuel is consumed during takeoff, resulting in a weight drop), but it still is a value greater than the TOGW of SpaceShipTwo. Consequently, to keep the wing loading low for the pull-up maneuver, the wing planform area must be increased.

Finally, the solution space also enables the comparison of the slenderness τ of the two launch systems. The slenderness parameter for SpaceShipTwo was determined to be overestimated by 7.6%, with a value 0.189 [45]. On the other hand, the slenderness parameter for Aspiration was smaller and with a value of 0.162. The slenderness parameters for both vehicles fall within their expected range in Figure 3.6. Even when the

slenderness parameter of SpaceShipTwo is corrected to account for the overestimation (i.e., $\tau = 0.176$), it can be observed that SpaceShipTwo possesses a higher slenderness parameter, resulting in a stouter vehicle geometry. This conclusion is not surprising since, after all, Aspiration is a lifting body vehicle, meaning that it possesses the highest volumetric efficiency of all vehicle geometries. Thus, the higher volumetric efficiency of Aspiration translates to a smaller slenderness parameter.

Moving forward, a sizing comparison between the SSTO vehicle solution and the two TSTSO vehicle solutions can also be performed. However, given the nature of their missions, their dimensional results would be significantly different. As it can be expected, the required TOGW for an orbital vehicle was several orders of magnitude higher than for the sub-orbital vehicles due to the increase in the fuel requirement. Thereafter, as the weight increases, the same low wing loading consideration for the wing sizing based on the pull-up and other turn maneuvers, will lead to higher planform area calculations. The only valuable comparison would be with their respective slenderness parameters, as this value is non-dimensional. As previously mentioned, the developed SSTO wing-body vehicle has a slenderness parameter of 0.173. This τ value is fairly close to the slenderness parameter of SpaceShipTwo as both vehicles are, in essence, wing-body geometries. For the same reason, the slenderness parameter of Aspiration is found to be lower than the slenderness parameter of the SSTO vehicle and SpaceShipTwo.

A more valuable comparison for the developed SSTO RBCC vehicle would be comparing it with another orbital vehicle that has a different propulsion system, staging process, and/or geometry. For instance, Figure 4.6 on the following page presents the solution space of a SSTO all-rocket vehicle with HTHL capabilities. From this figure, it

can be seen that the SSTO all-rocket vehicle estimates a lower TOGW but a greater wing planform area compared to the developed SSTO RBCC vehicle. The greater TOGW for the RBCC vehicle can be attributed to its fuel fraction. Using the trajectory constraints of Skylon as a reference, the fuel fraction was identified to be along the 0.7 margin. On the other hand, the fuel fraction for the all-rocket vehicle was identified to be at a lower margin of 0.5 [47]. Thus, a higher fuel fraction for the combined cycle vehicle translates to a greater TOGW. Additionally, assumptions for the structural weight parameters (i.e., the use of metals rather than composite materials and vice versa) for the weight budget equation can also affect the TOGW estimations.

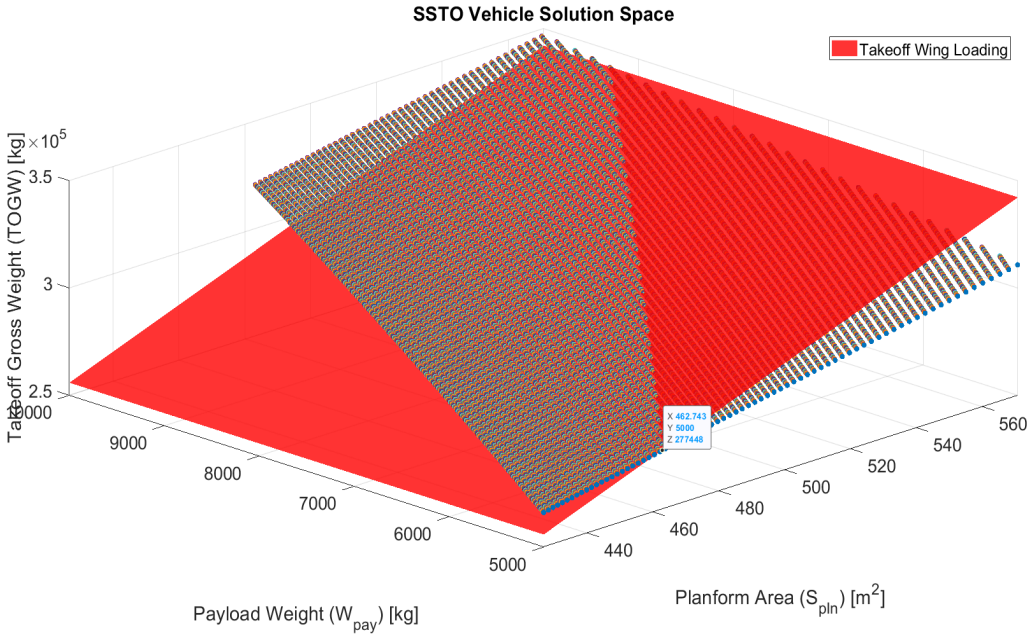

Figure 4.6: Solution Space of a SSTO All-Rocket Vehicle [47]

Similarly, comparing Figure 4.4 and Figure 4.6 allows the conclusion that the SSTO all rocket vehicle possesses a bigger planform area than the developed SSTO RBCC vehicle. This behavior for these two specific configurations can be explained based on the selected geometries. As it has been mentioned before, the modeled vehicle in this report

was derived from Skylon's wing-body configuration. On the other hand, the SSTO all-rocket vehicle being considered possesses an all body or lifting body geometry. A lifting body configuration is a configuration where no wing exists or is heavily required (i.e., low aspect ratio) as the vehicle body is shaped in a way that it can generate lift [41,48]. To achieve a low aspect ratio, the area of the wing must be bigger than the wingspan. Consequently, it is this geometrical difference that is causing the difference in magnitude for the planform areas in the solution space. A similar vehicle geometry should lead to similar planform areas for a more direct comparison and linear comparison of the TOGW.

At the end of the day, the most prominent design is the one that limits the operational costs of the vehicle. In general, the higher the TOGW, the higher the operational cost, and, as a result, the higher the ticket price for a given sub-orbital or orbital mission. Then, the higher the ticket price, the fewer the number of passengers willing (or capable) to pay for the experience, and the harder it is for a given company to break even and start earning profits. Consequently, the final comparison that was performed between the analyzed SSTO vehicles was through a 1st order correlation of the ticket price to TOGW ratio for a baseline mission of six passengers. Currently, Virgin Galactic has a ticket price of $250,000 for its 41,491 kg TSTSO system [10]. Consequently, the correlation of ticket price and TOGW for sub-orbital flights was of $6.025/kg. Hence, a 1st order estimation of the ticket price for Aspiration with its 23,221 kg TOGW is of $139,915.89.

On the other hand, it was mentioned in the introduction that Dennis Tito paid $20 million for his ticket to the International Space Station in 2001 [6]. Tito's flight occurred via a TSTSO system consisting of the Russian Soyuz-U launch vehicle (TOGW of 7,120 kg) and the Soyuz TM-32 spacecraft (313,000 kg) [49,50]. Hence, the total TOGW for the

mission was 320,120 kg. It must be noted that the TOGW of this TSTO system is greater than that of the SSTO RBCC vehicle. Thereafter, the correlation of ticket price to TOGW for orbital flights was determined to be $62.477/kg. Applying the developed hypersonic convergence model for the SSTO RBCC vehicle with a payload weight equivalent to 6 passengers resulted in a TOGW of 304,300 kg (planform area of 338 m^2). Consequently, with the derived 1st order correlation of the ticket price to TOGW, the ticket price for the SSTO RBCC vehicle was determined to be $19,011,620.64. This ticket price is slightly lower than the one paid by Tito. However, the TOGW for Tito's ticket price was derived under the assumption that the flight did not carry any additional payload as this information was not provided in the literature review. Including any additional payload will result in a higher TOGW that would then decrease the magnitude of the developed correlation, resulting in a decrease in the ticket price. On the other hand, the TOGW for the all-rocket vehicle was identified to be 277,500 kg (planform area of 462 m^2 and, once again, a smaller TOGW due to its lower fuel fraction), resulting in a ticket price of $17,337,248.53 [47]. Finally, Table 4.4 shown below, summarizes the parametric characteristics of the two sub-orbital vehicles and the two orbital vehicles for a baseline mission of 6 passengers. The same τ discussion that was introduced for the sub-orbital vehicles (i.e., wing-body geometry vs. lifting body geometry) is also applicable for the orbital vehicle designs.

Table 4.4: Comparison of the Parametric Requirements for a 6 Passenger Mission to Sub-Orbit and Orbit

Parameter	TSTSO SpaceShipTwo	SSTSO Aspiration	SSTO RBCC Vehicle	SSTO All-Rocket Vehicle
TOGW (kg)	41,491	23,221	304,300	277,500
S_{pln}(m^2)	47	74	338	462
Ticket Price ($)	250,000	139,915.89	19,011,620.64	17,337,248.53
Slenderness (-)	0.176	0.162	0.173	0.270
Geometry	Wing Body	All Body	Wing Body	All Body

CHAPTER 5

CONCLUSION

This project focused on the development of the solution space of a SSTO RBCC vehicle with HTHL capabilities for space tourism (through a parametric sizing analysis), and its subsequent comparison with other sub-orbital and orbital vehicle designs. After introducing the concept of space tourism and SSTO vehicles, the hypersonic convergence methodology was derived for the required PS analysis. From the derived methodology, a mathematical hypersonic convergence model was developed through the MATLAB interface. The model results were verified using Reaction Engines' Skylon spaceplane as a reference. The results of the model were found to be within a 5% error with respect to the theoretical values from the literature review.

With a verified model, the solution space of the SSTO RBCC vehicle was compared with two sub-orbital vehicle designs (a TSTSO wing-body vehicle and a SSTSO rocket powered lifting body vehicle) and an orbital vehicle design (a SSTO all-rocket vehicle) for space tourism. A comparison between the two sub-orbital vehicles for a baseline mission of six passengers indicated that the SSTSO vehicle required a smaller TOGW than the TSTSO vehicle. Additionally, it was identified that the SSTSO vehicle had a bigger planform area and a lower slenderness parameter than the TSTSO vehicles due to their geometrical characteristics. Given their mission differences, the developed SSTO vehicle had a greater TOGW and planform area than both sub-orbital vehicles. As a result, the designed SSTO RBCC vehicle was compared with a SSTO (all-rocket) vehicle

for more accurate and useful results.

The developed RBCC vehicle had a wing-body geometry, while the all-rocket vehicle had a lifting body geometry. Consequently, the comparison between the SSTO vehicles indicated that the RBCC vehicle required a higher TOGW but smaller planform area than the all-rocket vehicle. The higher TOGW requirement for the RBCC vehicle was caused by the higher fuel fraction (about a 0.1 margin) that the vehicle requires for a given mission. On the other hand, the lower planform area requirement for the RBCC vehicle was caused by their geometrical differences as a lifting body requires a higher planform to keep a low aspect ratio. Thereafter, it was identified from a 1st order ticket price to TOGW correlation that the wing-body RBCC vehicle has a higher ticket price than the lifting body all-rocket vehicle due to its higher TOGW.

Finally, this analysis allows us to conclude that SSTSO vehicles are more efficient than TSTSO vehicles for space tourism due to their smaller TOGW and to the fact that they do not require to reach orbital velocities. On the other hand, with current technology, TSTO vehicles appear to be a better option for space tourism applications than SSTO vehicles. It is true that SSTO systems have a lower TOGW requirement than TSTO systems. However, the staging process allows the TSTO system to decrease its mass significantly at high altitudes, resulting in a decrease in its required orbital velocity. On the other hand, the advantage of a lower TOGW from the SSTO vehicle is lost at higher altitudes as the vehicle has to carry “dead weight”, resulting in a higher required orbital velocity. Single-stage-to-orbit vehicles are possible (although maybe not optimal) with current technology. However, if future technologies provide a feasible solution for the high weight penalties,

then SSTO vehicles might finally have their chance to prove their worth for space tourism and other space activities.

APPENDIX A

MATLAB SCRIPT OF THE 2-D SOLUTION SPACE FOR SKYLON

```
%Code by Henry Barahona M.
%Objective: Solution Space for Skylon
%Last Modified: May 2, 2021

clc
clear
close all
tic

tauM=[0.12:0.001:0.30];
l=length(tauM);

for i=1:l
tau=tauM(1,i);
Spln=400; %Initial Guess of Planform Area
TOGWi=2.9E5; %Initial Guess of TOGW
x0 = [Spln TOGWi];
options = optimoptions('fsolve','MaxFunctionEvaluations',10000);
x = fsolve(@(x)HC(tau,x),x0);
Spln_M(i)=x(1);
TOGW_M(i)=x(2);
end

clc
figure('color','w')
plot(Spln_M,TOGW_M,'-k','LineWidth',1.5)

% Constraints
Vr=155; %Takeoff Velocity from Skylon Manual
rho=1.2250; %density of air at sea level
Cl_TO=0.60; %Lift Coefficient for T/O

WS = 0.5*rho*Vr^2*Cl_TO; %Wing Loading
S = 150:1:450;
W = WS.*S;
M = W/9.807;
hold on
plot(S,M,'-r','LineWidth',1.5);
axis([150 450 2.6E5 3.6E5])
xlabel('Planform Area (S_p_l_n) [m^2]')
ylabel('Takeoff Gross Weight (TOGW) [kg]')
title('Solution Space of a SSTO Vehicle with a RBCC Engine')
plot(361, 3.25E5,'db','MarkerSize',8,'MarkerFaceColor','b')
legend('Hypersonic Convergence Results', 'Takeoff Wing Loading Constraint', 'Design Point', 'Location',
'NW')
toc

function Eqn=HC(tau,x)
Spln=x(1);
TOGW=x(2);

%%Standard Atmos Constants
k=1.4;
R=287;
T0=288.15;
Re=6370E3;
```

```
g0=9.807;
rho0=1.2250;

%%Weight Constants for Weight Budget
Npax=20;
Ncrw=1;
Wpay=45*Npax;
Istr=21;
Cun=2.1;
Cun=Cun*(2000/2.205);
fmnd=1.05;
fmnd=fmnd*(2000/2.205);
fsys=0.16;
ETW=25;
fprv=0.50;
fprv=fprv*(2000/2.205);
fcrw=0.15;
fcrw=fcrw*(2000/2.205);

%%Volume Constants for Volume Budget
Vun=7.0;
kfcrw=12;
kvs=0.04;
kve=0.40;
kve=kve/(2000/2.205);
kvv=0.15;
rho_pay=130;
kcrw=2.0;

%%Trajectory Constants
%Air-Breathing Analysis
hi1=0; %initial altitude from data in manual
hf1=28; %final altitude from data in manual
Mi1=0; %initial Mach number from data in manual
Mf1=5.5; %final Mach number from data in manual
hi1_ft=hi1*10^3*3.28;
hf1_ft=hf1*10^3*3.28;
[thetai1 sigmai1]=STD_ATMOS(hi1_ft);
[thetaf1 sigmaf1]=STD_ATMOS(hf1_ft);
Ti1=thetai1*T0;
Tf1=thetaf1*T0;
Vi1=Mi1*sqrt(k*R*Ti1);
Vf1=Mf1*sqrt(k*R*Tf1);
delV1=Vf1-Vi1;
Isp1=50000/g0; %average Isp from data in manual
WR1=exp(delV1/(g0*Isp1));

%Rocket Analysis
hi2=28; %initial altitude from data in manual
hf2=90; %final altitude from data in manual
Mi2=5.2; %initial Mach number from data in manual
Mf2=27.8; %final Mach number from data in manual
hi2_ft=hi2*10^3*3.28;
hf2_ft=hf2*10^3*3.28;
[thetai2 sigmai2]=STD_ATMOS(hi2_ft);
[thetaf2 sigmaf2]=STD_ATMOS(hf2_ft);
```

```
Ti2=thetai2*T0;
Tf2=thetaf2*T0;
Vi2=Mi2*sqrt(k*R*Ti2);
Vf2=Mf2*sqrt(k*R*Tf2);
delV2=Vf2-Vi2;
Isp2=4500/g0; %from data in manual
WR2=exp(delV2/(g0*Isp2));

WR=WR1*WR2;
ff=1-1/WR;
TW0=2;
E_TW=13.2857;

%%Propulsion Constants
OF_ratio=6;  % Oxidzer to fuel Ratio
rhoOX=1141;  % Density of Liquid O2 (oxidizer)
rhoFuel=71; % Denisty of Liquid H2 (fuel)
rho_ppl=rhoFuel*(1+OF_ratio)/(1+OF_ratio*rhoFuel/rhoOX);

Vtot=tau*Spln^(1.5);
Kw=exp(0.081*(log(tau))^2-0.461*log(tau)+1.738)*tau;
Swet=Kw*Spln;

%Weight Budget Calculations
Wstr=Istr*Swet;
Csys=Cun+fmnd*Ncrw;
Wcew_prv=(1+fprv*Ncrw);
Wcrw=fcrw*Ncrw;

%Volume Budget Calculations
Vfix=Vun+kfcrw*Ncrw;
Vsys=Vfix+kvs*Vtot;
Vvoid=kvv*Vtot;
Vpay=Wpay/rho_pay;
Vcrw=(5.0+kcrw*Ncrw);

mu_a = 0.15;

%Weight Budget
W_OEW_N=(Istr*Kw*Spln)+Csys+(TW0*WR/(E_TW))*(Wpay+Wcrw);
W_OEW_D=((1/(1+mu_a))-fsys)-(TW0*WR/(E_TW));
W_OEW=W_OEW_N/W_OEW_D;
OWE=W_OEW+Wpay;

%Volume Budget
W_OWE_N=Vtot*(1-kvs-kvv)-Ncrw*(kfcrw-kcrw)-Vpay;
W_OWE_D=((WR-1)/rho_ppl)+(kve*TW0*WR);
W_OWE=W_OWE_N/W_OWE_D;

%Convergence Equation
Eqn(1)=OWE-W_OWE;
Eqn(2)=TOGW-OWE*WR;
end
```

APPENDIX B

MATLAB SCRIPT OF THE 3-D SOLUTION SPACE FOR A SSTO RBCC VEHICLE

```
%Code by Henry Barahona M.
%Objective: Solution Space for a SSTO RBCC Vehicle
%Last Modified: May 2, 2021

clc
clear
close all
tic
FS = 16;

%Define HC Input Variable Ranges
tau = 0.12:0.01:0.35;
Wpay = 50:25:2000;

L1=length(tau);
L2=length(Wpay);

for i = 1:L1
   for j = 1:L2;
   K_w=exp(0.081*(log(tau(i))^2)-0.461*log(tau(i))+1.738)*tau(i);
   Spln i=400;
   [Spln(i,j),TOGW(i,j),OEW(i,j),OWE(i,j)] = HC_SSTOF(tau(i), K_w, Spln i, Wpay(j));
   Swet(i)=K_w*Spln(i,j);
   end
end

%% Solution Space Constraint Analysis
%Takeoff Wing Loading
Smin = min(min(Spln));
Smax = max(max(Spln));
dS = (Smax-Smin)/length(tau);
Smax = Smax-dS;
Vr = 155;
rho = 1.2250;
CL_TO = 0.6;
q = 1/2*rho*Vr^2;
WS_TO = q*CL_TO;
S = Smin:dS:Smax;
W = WS_TO*S;
Mi = W/9.807;
for i = 1:length(tau)
   for j = 1:length(W_pay)
      M_TO(i,j) = Mi(i);
   end
end

%TO Constraint
figure('color','w')
hold on
TO = mesh(S, W_pay, M_TO.', 'FaceColor','r','FaceAlpha',0.8,'EdgeColor','none');

%Solution Space
for i = 1:length(Wpay)
   Spln_i = Spln(:,i);
   mesh(Spln_i, Wpay, TOGW.')
end
```

```
set(findall(gcf,'-property','FontSize'),'FontSize',FS)
title('3-D Solution Space for a SSTO Vehicle with a RBCC Engine')
legend(TO,{'Takeoff Wing Loading Constraint'})
view(-45, 45);
grid on
xlim([Smin 400])
xlabel('S_{pln} [m^2]')
ylabel('Payload Weight (W_{pay}) [kg]')
zlabel('TOGW [kg]')
toc

function [Spln_con, TOGW_conv, OEW, OWE2] = HC_SSTO(tau, Kw, Splni, Wpay)
%% Inputs
tau_e=tau;
Kw_e=Kw;
ff=0.68;

%% Constants
w_den=0.7096;
OF_ratio=6;
rhoFuel=71;
rhoOX=1141;
rho_ppl=rhoFuel*(1+OF_ratio)/(1+OF_ratio*(rhoFuel/rhoOX));
WR=1/(1-ff);
E_TW = 13.2857;
Cun=2.1;
Cun=Cun*(2000/2.205);
fmnd=1.05;
fmnd=fmnd*(2000/2.205);
Ncrw=1;
Csys=Cun+fmnd*Ncrw;
fcprv=45;
Wcprv=fcprv*Ncrw;
TW0=2;
Istr = 21;
fcrw=0.15;
fcrw=fcrw*(2000/2.205);
Wcrw=fcrw*Ncrw;

% Volume budget
kvv=0.15;
kvs=0.04;
kve=0.40;
kve=kve/(2000/2.205);
kcrw=2;
Vpa=Wpay/130;
Vcprv=5;
Vcrw=(Vcprv+kcrw*Ncrw);
kfcrw=12;
Vun=7;
Vfix=Vun+kfcrw*Ncrw;
Vfix=0;

%Volume Budget
C1v=1-kvv-kvs;
C2v=Vfix+(kfcrw-kcrw)*Ncrw;
```

```
C3v=Vpay;
C4v=(WR-1)/rhoppl;
C5v=kve*TW0*WR;
C6v=Wpay;
C7v=fcrw*Ncrw;

%Weight Budget
C1w=Istr;
C2w=Csys+Wcprv+((TW0*WR)/E_TW)*(Wpay+Wcrw);
C3w=w_den-((TW0*WR)/E_TW);

%% Convergence logic
conv=@(S_pln) ((C1w*Kw_e*S_pln+C2w)/(C3w))-(((tau_e*S_pln^1.5*C1v-C2v-C3v)/(C4v+C5v))-C6v-
C7v);
Spln_con=fzero(conv,Splni);

OEW=((C1w*Kw_e*Spln_con+C2w)/(C3w));
OWE2=(((tau_e*Spln_con^1.5*C1v-C2v-C3v)/(C4v+C5v))-C6v-C7v);

TOGW_conv=WR*(OEW+Wpay+Wcrw);
end
```

REFERENCES

[1] Mai, T. First Human Entered Space. *The National Aeronautics and Space Administration*. https://www.nasa.gov/directorates/heo/scan/images/history/April1961.html.

[2] Majority of Americans Believe Space Exploration Remains Essential. *Pew Research Center Science & Society*. https://www.pewresearch.org/science/2018/06/06/majority-of-americans-believe-it-is-essential-that-the-u-s-remain-a-global-leader-in-space/.

[3] Griffin, M. The Real Reasons We Explore Space. Air & Space Magazine, Jul 01, 2007.

[4] Wiles, J. Why We Explore. *The National Aeronautics and Space Administration*. https://www.nasa.gov/exploration/whyweexplore/why_we_explore_main.html.

[5] Graham, A. *Air Transport: A Tourism Perspective*. Elsevier, Amsterdam, 2019.

[6] von der Dunk, F. G. Space for Tourism? - Legal Aspects of Private Spaceflight for Tourist Purposes. Presented at the 57th International Astronautical Congress, Valencia, Spain, 2006.

[7] Space Tourism: 5 Companies That Will Make You An Astronaut. Revfine.com, Jun 20, 2020.

[8] Solovyov, D. "Russia Halts Space Tours as U.S. Retires Shuttle." *Reuters*, Mar 03, 2010.

[9] "Astronaut Buzz Aldrin's Vision of Space Tourism for the Masses." *CNN*, Aug 06, 2013.

[10] Learn - Virgin Galactic. https://www.virgingalactic.com/learn/.

[11] Kelly, J. W., Rogers, C. E., Brierly, G. T., Martin, J. C., and Murphy, M. G. Motivation for Air-Launch: Past, Present, and Future. In *AIAA SPACE and Astronautics Forum and Exposition*, American Institute of Aeronautics and Astronautics, 2017.

[12] Sheetz, M. "Virgin Galactic Stock Falls After Test Flight Delays Push Back Debut of Space Tourism Service." *CNBC*, Feb 26, 2021.

[13] Nicolai, L., and Carichner, G. *Fundamentals of Aircraft and Airship Design*. American Institute of Aeronautics and Astronautics, Inc, Restin, Virginia, 2010.

[14] Chudoba, B. *Lab #2: Parametric Sizing (PS) Process*. University of Texas at Arlington, Arlington, TX, 2020.

[15] Coleman, G. J. "Aircraft Conceptual Design - An Adaptable Parametric Sizing Methodology." 2010.

[16] Nield, G. *Final Environmental Assessment for the Launch and Reentry of SpaceShipTwo Reusable Suborbital Rockets at the Mojave Air and Space Port*. Federal Aviation Administration, Washington, DC, 2012.

[17] Hudson, G. History of the Phoenix VTOL SSTO and Recent Developments in Single-Stage Launch Systems.

[18] Stemler, J., Bogar, T., Farrell, D., Hunt, J., and Bulman, M. Assessment of RBCC-Powered VTHL SSTO Vehicles. Presented at the 9th International Space Planes and Hypersonic Systems and Technologies Conference and 3rd.Weakly Ionized Gases Workshop, Norfolk, VA, 1999.

[19] Longstaff, R., and Bond, A. The SKYLON Project. Presented at the 17th AIAA International Space Planes and Hypersonic Systems and Technologies Conference, San Francisco, CA, 2011.

[20] Ehrlich, C. Why the X-33 VentureStar Gave SSTO a Bad Name. Presented at the AIAA SPACE 2009 Conference & Exposition, Pasadena, California, 2009.

[21] Loftin, L. *Subsonic Aircraft: Evolution and the Matching of Size to Performance*. National Aeronautics and Space Administration, 1980.

[22] Roskam, J. *Airplane Design Part I: Preliminary Sizing of Airplanes*. Roskam Aviation and Engineering Corporation, Ottawa, Kansas, 1985.

[23] Cunningham, M. J., Freeman Jr., D. C., Wilhite, A. W., and Powell, R. W. Thrust Vectoring for Single-Stage-To-Orbit, Horizontal Takeoff, Horizontal Landing, Space Vehicles. Presented at the AIAA/ASME/SAE/ASEE 22nd Joint Propulsion Conference, Huntsville, Al, 1986.

[24] Tomita, N., Nebylov, A., Sokolov, V., Tsurumaru, D., Saotome, T., and Ohkami, Y. *Feasibility Study of a Rocket-Powered HTHL-SSTO with Ekranoplane as Takeoff Assist*. American Institute of Aeronautics and Astronautics, 1996.

[25] Curran, E. T., and Murthy, S. N. B. *Scramjet Propulsion*. American Institute of Aeronautics and Astronautics, 2000.

[26] Crocker, A. M., Cannon, J. H., and Andrews, D. G. A Comparison of Horizontal Takeoff RLVs for Next Generation Space Transportation. Presented at the 39th AIAA/ASME/SAE/ASEE Joint Propulsion Conference and Exhibit, Huntsville, Al, 2003.

[27] Dissel, A., Kothari, A., Raghavan, V., and Lewis, M. J. Comparison of HTHL and VTHL Air-Breathing and Rocket Systems for Access to Space. Presented at the 40th AIAA/ASME/SAE/ASEE Joint Propulsion Conference and Exhibit, Fort Lauderdale, Fl, 2004.

[28] Froning, H. D. Single-Stage HTHL Spaceplane Requirements for Orbital and Sub-Orbital Hypersonic Space Tourism Flight. Presented at the 14th AIAA/AHI Space Planes and Hypersonic Systems and Technologies Conference, 2006.

[29] Nakane, M., Kobayashi, D., Yoshida, H., and Ishikawa, Y. Feasibility Study on Single Stage to Orbit Space Plane with RBCC Engine. Presented at the 16th AIAA International Space Planes and Hypersonic Systems and Technologies Conference, 2009.

[30] Chudoba, B., Coleman, G., Oza, A., Gonzalez, L., and Czysz, P. A. *Solution-Space Screening of a Hypersonic Endurance Demonstrator*. Publication NASA/CR-2012-217774. NASA, 2012.

[31] Hempsell, M., and Longstaff, R. SKYLON Users' Manual. https://web.archive.org/web/20151129034506/http://www.reactionengines.co.uk/tech_docs/SKYLON_Users_Manual_Rev_2.1.pdf.

[32] Gong, C., Chen, B., and Gu, L. Design and Optimization of RBCC Powered Suborbital Launch Vehicle. Presented at the 19th AIAA International Space Planes and Hypersonic Systems and Technologies Conference, Atlanta, GA, 2014.

[33] Mehta, U., Aftosmis, M., Bowles, J., and Pandya, S. Skylon Aerodynamics and SABRE Plumes. Presented at the 20th AIAA International Space Planes and Hypersonic Systems and Technologies Conference, Glasgow, Scotland, 2015.

[34] Raymer, D. *Aircraft Design: A Conceptual Approach*. American Institute of Aeronautics and Astronautics, Reston, Virginia, 2018.

[35] Czysz, P. A., Claudio, B., and Chudoba, B. *Future Spacecraft Propulsion Systems and Integration Enabling Technologies for Space Exploration*. Springer Praxis Books, 2018.

[36] Maynard, I. Hypersonic Convergence Background and Methodology. Aerospace Vehicle Design (AVD) Laboratory University of Texas at Arlington (UTA).

[37] Ferretto, D., Fusaro, R., and Viola, N. *Innovative Multiple Matching Charts Approach to Support The Conceptual Design of Hypersonic Vehicles*. Institution of Mechanical Engineers, Torino, Italy, 2020.

[38] Hassan, M., Pfaender, H., and Mavris, D. Design Tools for Conceptual Analysis of Future Commercial Supersonic Aircraft. Presented at the AIAA Aviation 2020 Forum, Virtual Event, 2020.

[39] About OpenVSP. *OpenVSP*. http://openvsp.org/learn.shtml.

[40] Haley, J. OpenVSP Model for Skylon. http://hangar.openvsp.org/vspfiles/381.

[41] Chudoba, B., Rana, L., McCall, T., and Haley, J. A Parametric Sizing Study on the Effects of Configuration Geometry on a Lifting-Body Reentry Vehicle. Presented at the AIAA SPACE and Astronautics Forum and Exposition, Orlando, FL, 2017.

[42] Gudmundsson, S. *General Aviation Aircraft Design: Applied Methods and Procedures*. 2014.

[43] Lox/LH2. *Astronautix*. http://www.astronautix.com/l/loxlh2.html.

[44] Huang, X. *A Prototype Computerized Synthesis Methodology for Generic Space Access Vehicle (SAV) Conceptual Design*. University of Oklahoma, Norman, Oklahoma, 2006.

[45] Godziela, R. *Development of a Design Methodology for Synthesis of Virgin Galactic's SpaceShipTwo*. University of Texas at Arlington, 2020.

[46] Kinhekar, Sushrut. *Conceptual Design Process for a Single Stage to Sub Orbit Spaceplane for Space Tourism*. 2021.

[47] Vasquez, J. *Parametric Sizing of a Rocket SSTO Space Tourism Vehicle*. University of Texas at Arlington, Arlington, TX, 2021.

[48] Minami, Y., and Tsukamoto, T. A Subscale Flight Experiment for the Approach and Landing of a Lifting Body Re-Entry Vehicle. Presented at the 14th AIAA/AHI Space Planes and Hypersonic Systems and Technologies Conference, 2006.

[49] ISS Spacecraft: Soyuz TM. *SpaceRef.com*. http://www.spaceref.com/iss/spacecraft/soyuz.tm.html#:~:text=ISS%20Spacecraft%3A%20Soyuz%20TM&text=The%20overall%20mass%20of%20the,volume%20is%2010%20cubic%20meters.

[50] International Flight No. 222 Soyuz TM-32. *Human Spaceflights*. http://www.spacefacts.de/mission/english/soyuz-tm32.htm.

BIOGRAPHICAL INFORMATION

Henry J. Barahona Miranda is a senior at the University of Texas at Arlington who is pursuing an Honors Bachelor of Science in Aerospace Engineering and a minor in Mechanical Engineering. During his time at UTA, Henry served as an officer for the local chapter of the engineering honor society Tau Beta Pi and worked as a tutor and Supplementary Instruction (SI) leader to serve the community. Additionally, Henry has been awarded multiple awards and scholarships such as the Dean's List recognition, the Outstanding Aerospace Engineering Junior Award, and the Zodiac Aerospace Scholarship Endowment awarded by the Department Chair of the Mechanical and Aerospace (MAE) Department.

In addition to his senior design project, Henry has worked on several other projects, including the simple control solution for a traction motor used in hybrid vehicles, a supersonic airfoil design, the design of a propulsion system for two-stage to low earth orbit (LEO), and the forward dynamic simulation of a six degree of freedom rigid body. Additionally, Henry did undergraduate research on the impact of porosity in additively manufactured aircraft structures and participated in the NASA L'SPACE Mission Concept Academy (MCA) program, where, together with a team, he developed a preliminary design review (PDR). Finally, Henry plans to start working full-time after graduation and to pursue a M.S. in Aerospace Engineering.